A Recent Analytical Approach for Analysis of Sub-Synchronous Resonance in Doubly-Fed Induction Generator-Based Wind Farm

MOHAMED ABDEEN [1,2], HUI LI [1], SALAH KAMEL [3], AHMED KHALED[4], MAHMOUD EL-DABAH[2], MOHAMMED KHARRICH [5], AND HATEM FAIZ SINDI [6], (Senior Member, IEEE)

[1]State Key Laboratory of Power Transmission Equipment and System Security and New Technology, School of Electrical Engineering, Chongqing University, Chongqing 400044, China
[2]Department of Electrical Engineering, Faculty of Engineering, Al-Azhar University, Cairo 11651, Egypt
[3]Department of Electrical Engineering, Faculty of Engineering, Aswan University, Aswan 81542, Egypt
[4]Department of Electrical Engineering, Faculty of Engineering, Al-Azhar University, Qena 833523, Egypt
[5]Department of Electrical Engineering, Mohammadia School of Engineers, Mohammed V University, Rabat 10090, Morocco
[6]Department of Electrical and Computer Engineering, King Abdulaziz University, Jeddah 21589, Saudi Arabia

Corresponding authors: Mohamed Abdeen (abdeenm88@yahoo.com) and Hatem Faiz Sindi (hfsindi@kau.edu.sa)

ABSTRACT Sub-synchronous resonance (SSR) phenomenon occurs due to the interaction between wind turbine generators and series-compensated transmission lines. A doubly-fed induction generator (DFIG) is considered one of the most widely implemented generators in wind energy conversion systems. SSR analysis based on the eigenvalue method is the most important among the used methods. The accuracy of the eigenvalue method depends on the initial values of state variables. Previously, the initial values of the state variables were calculated based on the iterative approach which is suffering from convergence problem, lacking accuracy, and requiring a long computation time. Moreover, many steps and details haven't been provided. Consequently, it is urgent to fill this gap and show how can implement the SSR analysis model in detail. In this paper, a new application of a recent analytical approach is proposed for SSR analysis. All information is provided, and the SSR analysis model of a DFIG-based series compensated wind farm is built step-by-step. In order to prove the effectiveness and accuracy of the proposed method, the eigenvalue analysis based on the proposed and iterative methods is compared with the time-domain simulation results at different wind speeds and variable compensation levels. The results prove that the eigenvalue analysis based on the proposed method is more precise, where it is consistent with the simulation results in all studied cases. MATLAB software is used to validate the results.

INDEX TERMS Sub-synchronous resonance, DFIG-based series compensated wind farm, calculating the initial values, analytical approach, eigenvalue method, SSR analysis.

ABBREVIATIONS

SSR	Sub-Synchronous Resonance
DFIG	Doubly-Fed Induction Generator
FBM	First Benchmark Model
RSC	Rotor Side Converter
GSC	Grid Side Converter

NOMENCLATURE

f_s	Fundamental Frequency
f_n	Electrical Natural Frequency

K	Compensation Level (X_C/X_L)
X_C	Series Capacitor Reactance
X_L	Total Reactance of Transmission Line and Transformer
ρ	Air Density
A	Blade Sweep Area
R	Wind Turbine Rotor Radius
V_w	Wind Speed
C_P	Power Coefficient of the Blade
C_f	Wind Turbine Blade Design Constant
β	Pitch Angle
λ	Tip Speed Ratio of the Wind Speed
Ω_m	Mechanical Angular Velocity (rad/s).

T_e	Electromagnetic Torque of the Generator
T_m	Mechanical Torque of Wind Turbine
P_m	Mechanical Power of Wind Turbine
ω_t	Wind Turbine Shaft Speed
ω_r	DFIG Shaft Speed
T_g	Internal Torque of the Model
K_{tg}	Shaft Stiffness Coefficient of Drive Train
D_{tg}	Damping Coefficient between the Wind Turbine and Generator
D_g	Generator Damping Coefficient
D_t	Wind Turbine Damping Coefficient
H_g	Generator Inertia Constant
H_t	Wind Turbine Inertia Constant
ω_e	Synchronous Reference Frame Speed (1 p.u).
Ψ_{qm}, Ψ_{dm}	Airgap Flux Linkage Components in Quadrature and Direct-Axes
i_L	Transmission Line Current
v_c	Capacitor Voltage
v_s	Phase Generator Bus Voltage
E_B	Phase Infinite Bus Voltage
i_{qL}, i_{dL}	Transmission Line Current Components in Quadrature and Direct-Axes
v_{cq}, v_{cd}	Series Capacitor Voltage Components in Quadrature and Direct-Axes
v_{qs}, v_{ds}	Terminal Bus Voltage Components in Quadrature and Direct-Axes
v_{qr}, v_{dr}	DFIG Rotor Voltage Components in Quadrature and Direct-Axes
E_{Bq}, E_{Bd}	Infinite Bus Voltage Components in Quadrature and Direct-Axes
ω_b	Base Speed (2.pi.60 rad/s)
R_L	Transmission Line Resistance
i_{qs}, i_{ds}	DFIG Stator Current Components in Quadrature and Direct-Axes
i_{qr}, i_{dr}	DFIG Rotor Current Components in Quadrature and Direct-Axes
i_{0s}, i_{0r}	Zero Sequence Current Components of Stator and Rotor
v_{0s}, v_{0r}	Zero Sequence Voltage Components of Stator and Rotor
X_{ls}, X_{lr}	Stator and Rotor Leakage reactance
X_m	Magnetizing Reactance
X_s	Stator Reactance ($X_s = X_{ls} + X_m$)
X_r	Rotor Reactance ($X_r = X_{lr} + X_m$)
R_s, R_r	Stator and Rotor Resistances
ω_s	Synchronous Frame Frequency (2.pi.60 rad/s)
C_{DC}, V_{DC}	Capacitor and Voltage of DC-link
P_r	Power of Rotor Side Converter (RSC)
P_g	Power of Grid Side Converter (GSC)
i_{qg}, i_{dg}	Grid Side Converter Current Components in Quadrature and Direct-Axes
v_{qg}, v_{dg}	Grid Side Converter Voltage Components in Quadrature and Direct-Axes
v_g	Grid Side Converter Voltage
i_g	Grid Side Converter Current
X_{tg}	Grid Side Converter Reactance
Q_s	Reactive Power Delivery through DFIG Stator
Q_g, Q_g^{ref}	Reactive Power Delivery through Grid Side Converter and its Reference Value
FFT	Fast Fourier Transform
f_{FFT}	Frequency based on FFT
$f_{Pro.}$	Frequency based on the proposed method.
$f_{iter.}$	Frequency based on the iterative method

I. INTRODUCTION

Fixed series capacitor is inserted into a transmission line to increase the maximum transmittable power. Nevertheless, one of the reasons impeding the use of series capacitive compensation widely with wind farms is the potential threat of SSR, affecting the stability and safety of the entire system [1]. SSR phenomenon is a condition where the DFIG-based wind turbine exchanges energy with the series-compensated network at one or more frequencies less than the fundamental frequency. SSR occurs at high compensation levels and low wind speeds [1], [2].

Different methods have been presented for SSR analysis and they are: 1) time-domain simulation [3], [4], 2) frequency scanning [1], [5], and 3) eigenvalue analysis [6]–[10]. The latter method is the most important approach where it has been employed in several SSR studies [7]–[12]. The procedure of SSR analysis using the eigenvalue method has been presented in [6], [13]–[16]. However; 1) the authors have focused on the system modeling and they don't explain the process of calculating the initial values, 2) they have used the iterative approach to calculate the initial values, 3) most of the required data hasn't been provided. In [17], authors proposed an analytical approach that doesn't depend on any assumptions, requires less computation time, simple and easy to be implemented, the loss of DFIG back-to-back converter is considered and nonzero reactive power delivery through DFIG grid-side converter can be supported as well as no convergence problem. Consequently, the obtain initial values are accurate.

In this paper, a recent analytical approach is applied for SSR analysis. The main contributions of this work can be summarized in the following points:

– Accurate and simple recent analytical approach is proposed for SSR analysis based on the eigenvalue method.
– The modeling of DFIG-based wind farm interfaced with a series-compensated network in MATLAB/Simulink is built in detail.
– Eigenvalue analysis based on the proposed and iterative methods is compared with the time-domain simulation results at different wind speeds and variable compensation levels.

The rest of the paper is organized as follows. Power system description is presented in Section II. System modeling is introduced in Section III. Calculating the initial values of
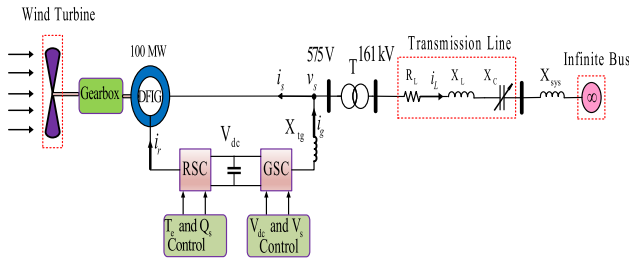
FIGURE 1. Studied system.

the state variables is conducted in Section IV. Eigenvalue analysis is carried out in Section V. SSR analysis is provided in Section VI. The summary is drawn in Section VII.

II. POWER SYSTEM DESCRIPTION

The studied system is shown in Fig.1, where the IEEE first benchmark model (FBM) is modified for studying the SSR phenomenon in a DFIG-based wind turbine instead of a synchronous generator [18]. In this study, one large DFIG represents a group of wind turbines. This technique has been widely used in several studies [2], [6], [11], [13]–[15], [19]–[21]. In this study, a 100 MW DFIG-based offshore wind farm is connected to an infinite bus through a 161-kV series compensated transmission line [22]. The rated voltage of DFIG is 575 V and the frequency is 60 Hz. The 100 MW wind farm is an aggregated model of 67 wind turbines, where the capacity of each wind turbine is 1.5 MW. The parameters of the single model and the aggregated model are provided in the Appendix.

III. SYSTEM MODELING

In order to study the impact of the SSR phenomenon on system stability, the studied system shown in Fig.1 has to be built using state-space equations as follows.

A. WIND TURBINE MODEL

The mechanical wind turbine torque is a strong function of the wind speed, and it is given as [23]:

$$T_m = \frac{0.5\rho A R C_P V_w^2}{\lambda} \tag{1}$$

The power coefficient of the blade is calculated as:

$$C_p = 0.5\left(\frac{RC_f}{\lambda} - 0.022\beta - 2\right)e^{-0.255(RC_f/\lambda)} \tag{2}$$

The tip speed ratio of the wind speed is defined by:

$$\lambda = \frac{\Omega_m R}{V_w} \tag{3}$$

Table 1 presents the relation between wind speed, rotor shaft speed, mechanical power, and shaft torque of the wind turbine. It should be noted that Table 1 represents the wind turbine model in the small-signal analysis procedure.

TABLE 1. Wind speed V_W, rotor shaft speed ω_m, mechanical power P_m, and shaft torque T_m lookup table.

$V_w\ (m/s)$	7	8	9	10	11	12
$\omega_m\ (p.u)$	0.8	0.88	0.97	1.07	1.18	1.2
$P_m\ (p.u)$	0.24	0.31	0.39	0.49	0.64	0.84
$T_m\ (p.u)$	0.3	0.35	0.4	0.46	0.54	0.7

B. SHAFT SYSTEM MODEL

A two-mass drive train model is widely used for studying the power system stability. The low-speed, wind turbine shaft speed, is represented by the first mass, whereas the high-speed, the DFIG shaft speed, is represented by the second mass. A two-mass system is expressed by state-space representation as [23], [24]:

$$
\frac{d}{dt}\overbrace{\begin{bmatrix} \omega_t \\ \omega_r \\ T_g \end{bmatrix}}^{\dot{X}} = \overbrace{\begin{bmatrix} \dfrac{-D_t - D_{tg}}{2H_t} & \dfrac{D_{tg}}{2H_t} & \dfrac{-1}{2H_t} \\ \dfrac{D_{tg}}{2H_g} & \dfrac{-D_g - D_{tg}}{2H_g} & \dfrac{1}{2H_g} \\ K_{tg}\omega_e & -K_{tg}\omega_e & 0 \end{bmatrix}}^{A_{shaft}} \overbrace{\begin{bmatrix} \omega_t \\ \omega_r \\ T_g \end{bmatrix}}^{X_{shaft}}
$$

$$
+ \overbrace{\begin{bmatrix} \dfrac{1}{2H_t} & 0 & 0 \\ 0 & \dfrac{-1}{2H_g} & 0 \\ 0 & 0 & 1 \end{bmatrix}}^{B_{shaft}} \overbrace{\begin{bmatrix} T_m \\ T_e \\ 0 \end{bmatrix}}^{U_{shaft}} \tag{4}
$$

where, the inputs of the shaft system model are T_e and T_m; whereas the state variables are ω_t, ω_r, and T_g. The constants of the two-mass model are K_{tg}, D_{tg}, D_g, D_t, H_g, H_t, and ω_e. All the parameters are in per-unit. Table 1 is used to obtain the optimal wind turbine torque T_m at any given wind speed, while T_e can be written in terms of the currents and airgap flux linkages of DFIG as follows:

$$\boldsymbol{T}_e = \boldsymbol{\psi}_{qm}\boldsymbol{i}_{dr} - \boldsymbol{\psi}_{dm}\boldsymbol{i}_{qr} \tag{5}$$

where, the airgap flux linkages is calculated as follows:

$$\boldsymbol{\psi}_{qm} = \boldsymbol{X}_m(\boldsymbol{i}_{qs} + \boldsymbol{i}_{qr}) \tag{6}$$
$$\boldsymbol{\psi}_{dm} = \boldsymbol{X}_m(\boldsymbol{i}_{ds} + \boldsymbol{i}_{dr}) \tag{7}$$

C. TRANSMISSION LINE MODEL

Although the dynamics in transmission networks are often ignored in power system studies, it is related to the SSR phenomenon. Thus, the transmission line is represented as a series RLC circuit. The dynamics equations per phase is described as [14]:

$$R_L.i_L + L\frac{di_L}{dt} + v_C = v_s - E_B \tag{8}$$

$$C\frac{dv_c}{dt} = i_L \tag{9}$$

The transmission line dynamics equations is described by state-space representation as:

$$\frac{d}{dt}\overbrace{\begin{bmatrix} i_{qL} \\ i_{dL} \\ v_{cq} \\ v_{cd} \end{bmatrix}}^{\dot{X}} = \overbrace{\begin{bmatrix} \dfrac{-R_L}{X_L} & -\mathrm{w}_e & \dfrac{-1}{X_L} & 0 \\ \mathrm{w}_e & \dfrac{-R_L}{X_L} & 0 & \dfrac{-1}{X_L} \\ X_C & 0 & 0 & -\mathrm{w}_e \\ 0 & X_C & \mathrm{w}_e & 0 \end{bmatrix}}^{A_{T.L}} \overbrace{\begin{bmatrix} i_{qL} \\ i_{dL} \\ v_{cq} \\ v_{cd} \end{bmatrix}}^{X_{T.L}}$$

$$+ \overbrace{\begin{bmatrix} \mathrm{w}_b & 0 & 0 & 0 \\ 0 & \mathrm{w}_b & 0 & 0 \\ 0 & 0 & 1 & 0 \\ 0 & 0 & 0 & 1 \end{bmatrix}}^{B_{T.L}} \overbrace{\begin{bmatrix} \dfrac{v_{qs} - E_{Bq}}{X_L} \\ \dfrac{v_{ds} - E_{Bd}}{X_L} \\ 0 \\ 0 \end{bmatrix}}^{U_{T.L}} \quad (10)$$

From the above equation, it is clear that the inputs are v_{qs}, v_{ds}, E_{Bq}, and E_{Bd}; and the state variables are i_{qL}, i_{dL}, v_{cq}, and v_{cd}. The value of X_C is changed according to the compensation level.

D. DFIG MODEL
A 6$^{\text{th}}$ order dynamic model is used for the DFIG with a rotor-side converter. The model is represented as [6]:

$$\dot{X} = A_{DFIG}X_{DFIG} + B_{DFIG}U_{DFIG} \quad (11)$$

where, X_{DFIG} represents the state variables, U_{DFIG} represents the inputs, B_{DFIG} represents the constants (Electrical parameters) and A_{DFIG} includes constants as well as one variable (rotor speed ω_r).

$$X_{DFIG} = [i_{qs}; i_{ds}; i_{0s}; i_{qr}; i_{dr}; i_{0r}] \quad (12)$$
$$U_{DFIG} = [v_{qs}; v_{ds}; v_{0s}; v_{qr}; v_{dr}; v_{0r}] \quad (13)$$

The subscripts *s, r, d, q,* and *0* denote on the stator side, the rotor side, the direct component, quadrature component, and zero sequence component, respectively. Since the system is balanced, the parameters i_{0s}, i_{0r}, v_{0s} and v_{0r} equal zero.

Eqs. (14) and (15), as shown at the bottom of the page. All variables and parameters are in per-unit except ω_b, ω_r, and ω_s are in rad/sec.

E. DC-LINK MODEL
In order to take the DC-link capacitor dynamics into consideration, the DC-link is derived as a first-order model as follows [6], [13]:

$$C_{DC}V_{DC}\frac{dV_{DC}}{dt} = P_r - P_g \quad (16)$$

The active powers of the rotor side converter P_r and grid side converter P_g are given as:

$$P_r = 0.5(v_{qr}i_{qr} + v_{dr}i_{dr}) \quad (17)$$
$$P_g = 0.5(v_{qg}i_{qg} + v_{dg}i_{dg}) \quad (18)$$

Since the inputs of the active powers, v_{qr}, v_{dr}, i_{qr}, i_{dr}, v_{qg}, v_{dg}, i_{qg} and i_{dg}, are in per-unit and the V_{DC} is actual value, the active power should be converted from per-unit to actual value by its multiplying with the base value.

F. INTEGRATED SYSTEM MODEL
Some additional algebraic equations are required to integrate the DFIG model with the transmission line model. To do so; **First**, the GSC current is calculated by applying KCL at a common point between the stator, GSC, and transmission line as shown in Fig.1. Thus, the following equation can be obtained [6]:

$$i_g = i_s + i_L \quad (19)$$

The *qd*-axis GSC currents can be written as:

$$i_{qg} = i_{qs} + i_{qL} \quad (20)$$
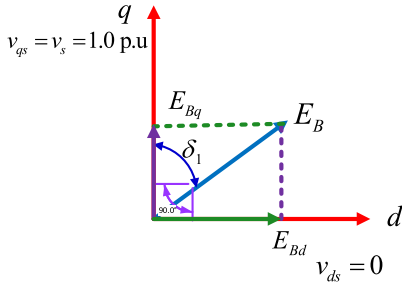$$i_{dg} = i_{ds} + i_{dL} \quad (21)$$

Second, KVL is applied at the same point to get the DFIG terminal voltage as:

$$v_g - v_s = jX_{tg}i_g \quad (22)$$

where, v_g is provided by GSC controllers.

$$B_{DFIG} = w_b \begin{bmatrix} X_s & 0 & 0 & X_m & 0 & 0 \\ 0 & X_s & 0 & 0 & X_m & 0 \\ 0 & 0 & X_{ls} & 0 & 0 & 0 \\ X_m & 0 & 0 & X_r & 0 & 0 \\ 0 & X_m & 0 & 0 & X_r & 0 \\ 0 & 0 & 0 & 0 & 0 & X_{lr} \end{bmatrix}^{-1} \quad (14)$$

$$A_{DFIG} = -B_{DFIG} \begin{bmatrix} R_s & \dfrac{w_s}{w_b}X_s & 0 & 0 & \dfrac{w_s}{w_b}X_m & 0 \\ -\dfrac{w_s}{w_b}X_s & R_s & 0 & -\dfrac{w_s}{w_b}X_m & 0 & 0 \\ 0 & 0 & R_s & 0 & 0 & 0 \\ 0 & \dfrac{w_s - w_r}{w_b}X_m & 0 & R_r & \dfrac{w_s - w_r}{w_b}X_r & 0 \\ -\dfrac{w_s - w_r}{w_b}X_m & 0 & 0 & -\dfrac{w_s - w_r}{w_b}X_r & R_r & 0 \\ 0 & 0 & 0 & 0 & 0 & R_r \end{bmatrix} \quad (15)$$

FIGURE 2. SSR analysis model.

The *qd*-axis terminal voltages is expressed as:

$$v_{qs} = v_{qg} - X_{tg}i_{dg} \qquad (23)$$

$$v_{ds} = v_{dg} + X_{tg}i_{qg} \qquad (24)$$

The stator reactive power is given by:

$$Q_s = 0.5\left(v_{qs}i_{ds} - v_{ds}i_{qs}\right) \qquad (25)$$

G. DFIG CONVERTER CONTROLLERS
In an atypical DFIG wind turbine, the vector control technique is used to control both the GSC and RSC [24]. In RSC controllers, Table 1 is used to obtain optimal torque, reference torque T_e^*, corresponding to the wind speed v_w as shown in Fig. 2. The value of reference reactive power Q_s^* can be set to fixed value or zero (unity power factor) [25]. In this study, Q_s^* is equal to zero. The parameters of PI controllers are listed in Appendix. SSR analysis model of DFIG-based wind turbine connected to a series compensated transmission line is shown in Fig.2.

IV. CALCULATING THE INITIAL VALUES OF THE STATE VARIABLES
The main goal of this procedure is to identify the initial values of the state vector X_0 under changing the operating point (varying the compensation level, $K = X_c/X_L$, and wind speed).

$$X_0 = [w_r \ w_t \ T_{tg} \ i_{qL} \ i_{dL} \ v_{cq} \ v_{cd} \ i_{qs} \ i_{ds} \ i_{qr} \ i_{dr} \ v_{DC}] \quad (26)$$

The initial value of V_{DC} equals 1150 V at any operating point. The initial values of shaft system, w_r, w_m or w_t and T_{tg}, can be obtained from Table 1 according to the given wind speed. The rest of the initial values can be obtained in three

FIGURE 3. System equivalent circuit in steady-state.

steps. The load flow analysis is conducted in step 1. The initial values of the transmission line and DFIG are obtained in steps 2 and 3, respectively.

Step 1: Load flow analysis

Fig.3 shows the equivalent circuit of the system in the steady-state, where the system consists of two buses, namely, PV and infinite. The generator bus (1), DFIG stator node, is treated as a PV bus where the voltage magnitude and active power are scheduled. The infinite bus (2) is treated as a slack bus where the voltage magnitude and phase angle are known [15].

The load flow analysis is expressed as:

$$P_k = \sum_{i=1}^{n} |Y_{ki}| \, |V_i| \, |V_k| \cos\left(\theta_{ki} + \delta_i - \delta_k\right) \qquad (27)$$

where, n is the number of buses; Y is admittance $Y = 1/Z_L$, $Z_L = (R_L) + \mathrm{J}\left(X_L + X_{sys} - X_C\right)$; P is the optimum active power at the generator bus corresponding to the given wind speed as given in Table 1; V is the voltage magnitude; the subscript k refers to bus 1 and subscript $i = 1, 2$.

It is assumed that the voltage magnitude at PV and slack buses equal 1, $E_B = V_s = 1$ p.u., and the angle at slack bus $\delta_2 = 0$.

FIGURE 4. The *dq* frame representation of DFIG and infinite bus voltage.

The load flow analysis is done to obtain the angle δ_1 at PV bus as follows:

$$\frac{R_L V_s}{R_L^2 + (X_L + X_{sys} - X_C)^2} - \frac{R_L V_s E_B}{R_L^2 + (X_L + X_{sys} - X_C)^2} \cos \delta_1$$
$$+ \frac{R_L V_s (X_L + X_{sys} - X_C)}{R_L^2 + (X_L + X_{sys} - X_C)^2} \sin \delta_1 - P_w = 0 \quad (28)$$

where, all these parameters are constant values at all cases except X_c and P_w which depend on the operating point. It should be noted that X_L in the above equation equals the transmission line reactance (0.5 p.u) plus transformer reactance (0.14 p.u). In order to illustrate this procedure, the operating point will be assumed. For instance, the compensation level and wind speed are 50 % ($X_C = 0.25\ p.u$) and 9 m/s ($P_w = 0.39\ p.u$), respectively. Using the above equation, δ_1 is 0.1761 rad. The initial values of the shaft system can be obtained from Table 1. ($w_r = w_m = 0.97\ p.u$, and $T_{tg} = T_e^* = 0.4\ p.u$.)

Step 2: Initial values of transmission line state variables (i_{qL}, i_{dL}, v_{cq} and v_{cd}).

In general, the *q*-axis of the synchronous rotating *qd* frame is assumed to be aligned with the stator voltage of DFIG v_s as shown in Fig.4.

The DFIG stator voltage components in quadrature and direct-axes is expressed as:

$$v_{qs} = v_s = E_B = 1 \text{ p.u} \quad (29)$$
$$v_{ds} = 0 \quad (30)$$

The infinite bus voltage components in direct and quadrature-axes is calculated as:

$$E_{Bd} = E_B \sin \delta_1 \quad (31)$$
$$E_{Bq} = E_B \cos \delta_1 \quad (32)$$

Based on δ_1 from the previous step, the infinite bus voltage components in *dq*-frame will be known values. Since the transmission line model includes four state variables, four equations are required. By setting the time derivates to zero (10), $\dot{x}$, the final four equations of the transmission line is given as:

$$\frac{-R_L}{X_L} i_{qL} - w_e i_{dL} - \frac{1}{X_L} v_{cq} + \frac{v_{qs} - E_B \cos \delta_1}{X_L} = 0 \quad (33)$$

$$w_e i_{qL} - \frac{R_L}{X_L} i_{dL} - \frac{1}{X_L} v_{cd} + \frac{v_{ds} - E_B \sin \delta_1}{X_L} = 0 \quad (34)$$

$$X_C i_{qL} - w_e v_{cd} = 0 \quad (35)$$
$$X_C i_{dL} + w_e v_{cq} = 0 \quad (36)$$

It should be noted that the angle δ_1 is in radian. The initial values of i_{qL}, i_{dL}, v_{cq}, and v_{cd} can be calculated using the MATLAB command FSOLVE. For instance, when wind speed is 9 m/s and compensation level is 50 %, δ_1 is 0.1761 rad as calculated in the previous step. Thus, $i_{qL0} = 0.4501, i_{dL0} = 0.0166, v_{cq0} = -0.0041$ and $v_{cd0} = 0.1125 p.u.$

Step 3: Initial values of DFIG state variables (i_{qs}, i_{ds}, i_{qr}, and i_{dr}).

Based on the transmission line currents, i_{qL} and i_{dL}, the stator and rotor currents of DFIG can be obtained as follows: the rotor currents, i_{dr} and i_{qr}, can be calculated through (37) and (38); then, the rotor voltages, v_{dr} and v_{qr}, can be obtained using (39) and (40); next, the quadrature axis of DFIG grid side converter current, i_{qg}, is determined based on (41); finally, the stator currents can be expressed by (45) and (46) [17]:

$$i_{dr} = \left(\frac{w_b R_s}{w_e X_m} + \frac{X_s v_{ds}}{X_m v_{qs}} \right) i_{qg} + \left(\frac{Q_g^{ref} X_s}{X_m v_{qs}} - \frac{w_b}{w_e X_m} v_{qs} \right.$$
$$\left. - \frac{w_b R_s}{w_e X_m} i_{qL} - \frac{X_s}{X_m} i_{dL} \right) = a_1 i_{qg} + b_1 \quad (37)$$

$$i_{qr} = \left(\frac{X_s}{X_m} - \frac{w_b R_s v_{ds}}{w_e X_m v_{qs}} \right) i_{qg} + \left(\frac{w_b}{w_e X_m} v_{ds} - \frac{X_s}{X_m} i_{qL} \right.$$
$$\left. + \frac{w_b R_s}{w_e X_m} i_{dL} - \frac{Q_g^{ref} w_b R_s}{w_e X_m v_{qs}} \right) = a_2 i_{qg} + b_2 \quad (38)$$

$$v_{qr} = \left(\frac{(w_e - w_r) X_m v_{ds}}{w_b v_{qs}} - a_2 R_r - \frac{(w_e - w_r) X_r a_1}{w_b} \right) i_{qg}$$
$$+ \left(\frac{(w_e - w_r) Q_g^{ref} X_m}{w_b v_{qs}} - \frac{(w_e - w_r) X_m}{w_b} i_{dL} \right.$$
$$\left. - b_2 R_r - \frac{(w_e - w_r) X_r b_1}{w_b} \right) = a_3 i_{qg} + b_3 \quad (39)$$

$$v_{dr} = \left(\frac{(w_e - w_r) X_r a_2}{w_b} - \frac{(w_e - w_r) X_m}{w_b} - a_1 R_r \right) i_{qg}$$
$$+ \left(\frac{(w_e - w_r) X_r b_2}{w_b} + \frac{(w_e - w_r) X_m}{w_b} i_{qL} - b_1 R_r \right)$$
$$= a_4 i_{qg} + b_4 \quad (40)$$

$$a_5 i_{qg}^2 + b_5 i_{qg} + c_5 = 0 \quad (41)$$

where:

$$a_5 = a_2 a_3 + a_1 a_4 \quad (42)$$

$$b_5 = -v_{qs} - \frac{v_{ds}^2}{v_{qs}} + a_3 b_2 + a_2 b_3 + a_4 b_1 + a_1 b_4 \quad (43)$$

$$c_5 = \left(-\frac{Q_g^{ref} v_{ds}}{v_{qs}} + b_2 b_3 + b_1 b_4 \right) \quad (44)$$

$$i_{qs} = -(i_{ql} - i_{qg}) \quad (45)$$

$$i_{ds} = -\left(i_{dl} - \frac{v_{ds}}{v_{qs}} i_{qg} - \frac{Q_g^{ref}}{v_{qs}} \right) \quad (46)$$

TABLE 2. The steady-state values of the system state variables for K = 50 % and V_ω = 9 m/s.

ω_{r0}	0.97	ω_{m0}	0.97	T_{tg0}	0.4
δ_1	0.1761	i_{qL0}	0.4501	i_{dL0}	0.0166
v_{cq0}	-0.0041	v_{cd0}	0.1125	i_{qs0}	-0.4705
i_{ds0}	-0.0166	i_{qr0}	0.4996	i_{dr0}	0.3662

TABLE 3. Eigenvalues of the entire system modes at 50 % compensation level and 9 m/s wind speed.

Mode	Description	Eigenvalue	Freq. (Hz)
$\lambda_{1,2}$	SSR	**2 ± j 188**	30
$\lambda_{3,4}$	Sup-syn.	-19.3 ± j 568.1	90.4
$\lambda_{5,6}$	Torsional	-0.5 ± j 2.1	0.33
$\lambda_{7,8}$	Electromech.	-57 ± j 19.4	3.08
$\lambda_{9,10}$	Very high freq.	-1788 ± j 889	141
$\lambda_{11,12}$	PI Controllers	-0.3± j 0.8	0.12
$\lambda_{13,14}$	PI Controllers	-0.0 ± j 0.0	0
λ_{15}	No oscillatory	-9	0
λ_{16}	No oscillatory	-2.1	0
λ_{17}	No oscillatory	-0.6	0
λ_{18}	No oscillatory	-0.1	0
λ_{19}	No oscillatory	-37	0
λ_{20}	No oscillatory	-48	0
λ_{21}	No oscillatory	-0.0	0
λ_{22}	No oscillatory	-0.0	0
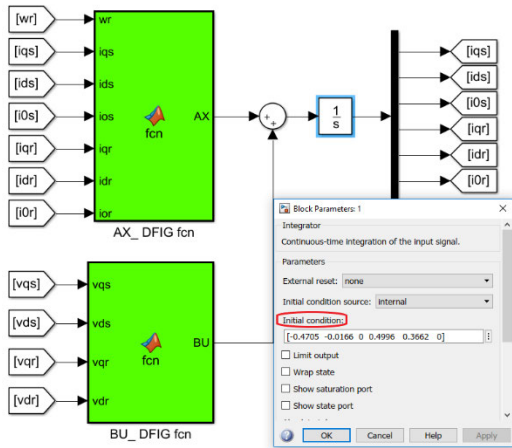
FIGURE 5. Initial values of DFIG model.

Table 2 presents the initial values of the system state variables at 50% compensation level and 9 m/s wind speed.

V. EIGENVALUE ANALYSIS

After building the entire system in MATLAB/Simulink as earlier explained and providing the initial values of the shaft system model, transmission line model, and DFIG model as shown in Fig.5, the file will be saved in the name of SSRDFIG.

It should be noted that the values of X_C in the transmission line model, and the rotor speed in the DFIG model has to be changed according to their values used in steps 2 and 3. For extracting the eigenvalue of the system at any operating point, the following two expressions have to be written in the MATLAB command as follows [13]:

$$\ll [\text{A B C D}] = \text{linmod ('SSRDFIG')}$$

$$\ll \text{eig(A)}$$

Since the system comprises of 22nd state variables, there are 22 modes as presented in Table 3.

VI. SSR ANALYSIS

In this section, eigenvalue analysis is carried out using the proposed method and iterative method with the aim of validating the effectiveness and accuracy of the proposed method. The obtained results of eigenvalue are compared with the time-domain simulation at different compensation levels and variable wind speeds.
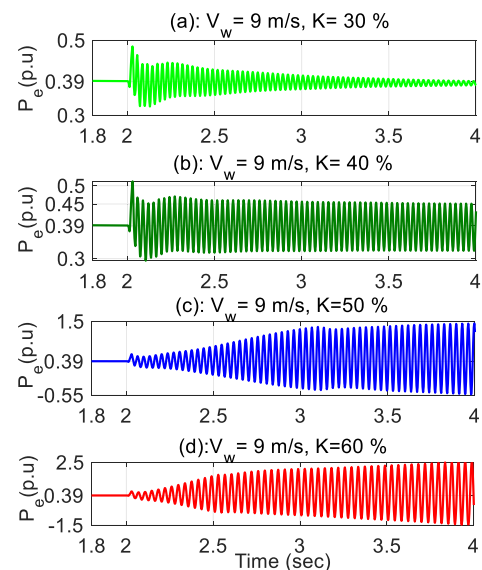

FIGURE 6. Electrical power dynamic response at constant wind speed and different compensation levels.

A. DIFFERENT COMPENSATION LEVELS

In what follows, the impact of different compensation levels on the system stability is studied using time-domain simulation, eigenvalue analysis based on the proposed method, and eigenvalue analysis based on the iterative method. Based on the time-domain simulation shown in Fig.6, the system loses its stability by increasing the compensation level. FFT analysis of electrical power signal at different compensation levels is conducted as shown in Fig.7 and listed in Table 4. The eigenvalue analysis based on the proposed and iterative methods is given in Table 4. Through comparing the FFT analysis with the eigenvalue analysis, the following notes can

TABLE 4. Frequency of the electrical power signal (P_e) based on FFT analysis (f_{FFT}), eigenvalue analysis based on the iterative method, eigenvalue analysis based on the proposed method at different compensation levels.

K %	f_{FFT}	Iterative Method [17]		Error %	Proposed Method		Error %
30	36.5 Hz	-1.0 ± j 226	36 Hz	1.38	-1.2 ± j 229	36.4 Hz	0.27
40	33 Hz	0.61 ± j 204	32.5 Hz	1.58	0.4 ± j 207	32.9 Hz	0.3
50	30 Hz	2.2 ± j 185	29.4 Hz	2	2 ± j 188	29.9 Hz	0.33
60	27.3 Hz	3.9 ± j168	26.7 Hz	2.2	3.7 ± j171	27.2 Hz	0.36
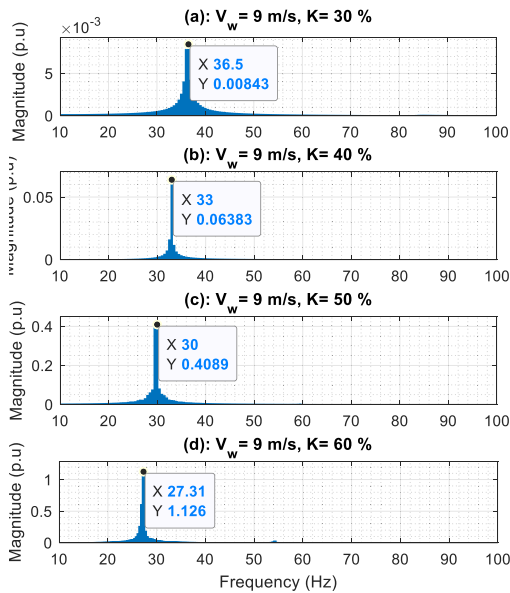
FIGURE 7. FFT analysis of electrical power signal at 9 m/s wind speed and different compensation levels.

FIGURE 8. Electrical power dynamic response at 50 % compensation level and different wind speeds.

be extracted from Table 4: 1) it is clear that the obtained frequency based on the proposed method almost equals the frequency of FFT analysis ($f_{FFT} = 36.5$ Hz, $f_{pro.} = 36.4$ Hz at 30 % compensation level). 2) the obtained frequency based on the iterative method is less than the FFT frequency ($f_{FFT} = 36.5$ Hz, $f_{iter.} = 36$ at 30 % compensation level). 3) the proposed method is more precise than the iterative method at all compensation levels. For example, the error based on the proposed method is around 0.36 % whereas the error based on the iterative method is around 2.2 % at 60 % compensation level.

B. DIFFERENT WIND SPEEDS

The effect of different wind speeds on the system stability is investigated using time-domain simulation, eigenvalue analysis based on the proposed method, and eigenvalue analysis based on the iterative method. Fig.8 shows that the system becomes more stable with increasing the wind speed. Fig. 9 displays the frequency of electrical power signal at different wind speeds based on the FFT analysis. The eigenvalue analysis based on the proposed and iterative methods is provided in Table 5. The following conclusions can be
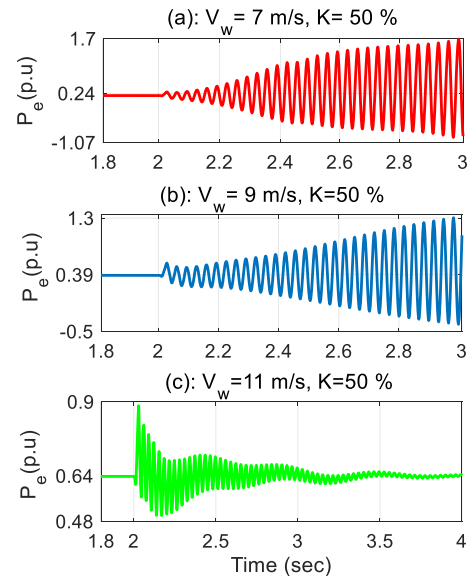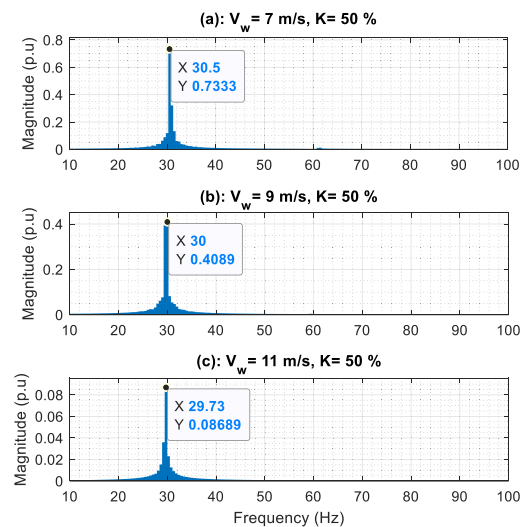

FIGURE 9. FFT analysis of electrical power signal at 50 % compensation level and different wind speeds.

drawn from Table 5: 1) the obtained frequency based on the proposed method is almost consistent with the frequency of FFT analysis ($f_{FFT} = 29.7$ Hz, $f_{pro.} = 29.6$ Hz at

TABLE 5. Frequency of the electrical power signal (P$_e$) based on FFT analysis (f_{FFT}), eigenvalue analysis based on the iterative method, eigenvalue analysis based on the proposed method at different wind speeds.

V$_w$	f_{FFT}	Iterative Method [17]		Error %	Proposed Method		Error %
7	30.5 Hz	**4.6± j 188**	29.9 Hz	1.15	**4.4± j 191**	30.4 Hz	0.32
9	30 Hz	**2.2± j 185**	29.4 Hz	2	**2± j 188**	29.9 Hz	0.33
11	29.7 Hz	-2± j 183	29 Hz	2.4	-2.2± j 186	29.6 Hz	0.33

11 m/s wind speed). 2) the obtained frequency based on the iterative method lacks accuracy where f_{FFT} = 29.7 Hz while $f_{iter.}$ = 29 Hz at 11 m/s wind speed. 3) the proposed method has better results compared with the iterative method at all wind speeds. For example, the error based on the proposed method is 0.33 % whereas the error based on the iterative method is 2.4 % at 11 m/s wind speed.

VII. CONCLUSION

In this paper, a recent analytical approach for calculating the initial values has been employed for SSR analysis. The analytical approach is accurate, simple, easy to be implemented, requires less computation time, and doesn't depend on any assumptions. Calculating the steady-state operating point of DFIG and extracting the system eigenvalue have been introduced step-by-step. The eigenvalue results of the proposed and iterative methods have been compared with the simulation results at different compensation levels and variable wind speeds. The results proved the superiority and accuracy of the proposed method compared with the iterative method in all studied cases, where the time-domain simulation is consistent with eigenvalue analysis based on the proposed method.

APPENDIX

DFIG PARAMETERS

Rated power	1.5 MW	100 MW
Rated voltage	575 V	575 V
Rated frequency	60 Hz	60 Hz
R_s	0.023	0.023
X_{ls}	0.18	0.18
R_r	0.016	0.016
X_{lr}	0.16	0.16
X_M	2.9	2.9
DC-link voltage	1200 V	1200 V
DC-link capacitor	10000 μF	67*10000 μF

Transmission line parameters

Transformer ratio	575 V/161 kV
Base power	100 MVA
R_L	0.02
X_L	0.5
X$_C$ at 50 % compensation level	64.8 ohm
X_T	0.14
$X_{Sys.}$	0.06

Drive train parameters

H_t	4.32 sec
H_g	0.685 sec
D_t	0
D_g	0
D_{tg}	1.5 p.u
K_{tg}	1.11

PI parameters of DFIG converter

K$_{P1}$	0.2	K$_{P5}$	0.1
K$_{i1}$	0.4	K$_{i5}$	2
K$_{P2}$	4	K$_{P6}$	0.08
K$_{i2}$	100	K$_{i6}$	0.5
K$_{P3}$	0.01	K$_{P7}$	0.1
K$_{i3}$	0.04	K$_{i7}$	2
K$_{P4}$	4	K$_{P8}$	0.08
K$_{i4}$	100	K$_{i8}$	0.5

REFERENCES

[1] K. Padiyar, *Analysis of Subsynchronous Resonance in Power Systems.* Boston, MA, USA: Kluwer Academic, 1999.

[2] H. A. Mohammadpour and E. Santi, "Sub-synchronous resonance analysis in DFIG-based wind farms: Definitions and problem identification—Part I," in *Proc. IEEE Energy Convers. Congr. Expo. (ECCE)*, Sep. 2014, pp. 812–819.

[3] M. Ghafouri, U. Karaagac, H. Karimi, S. Jensen, J. Mahseredjian, and S. O. Faried, "An LQR controller for damping of subsynchronous interaction in DFIG-based wind farms," *IEEE Trans. Power Syst.*, vol. 32, no. 6, pp. 4934–4942, Nov. 2017.

[4] M. Ghafouri, U. Karaagac, J. Mahseredjian, and H. Karimi, "SSCI damping controller design for series-compensated DFIG-based wind parks considering implementation challenges," *IEEE Trans. Power Syst.*, vol. 34, no. 4, pp. 2644–2653, Jul. 2019.

[5] M. Bongiorno, J. Svensson, and L. Angquist, "Single-phase VSC based SSSC for subsynchronous resonance damping," *IEEE Trans. Power Del.*, vol. 23, no. 3, pp. 1544–1552, Jul. 2008.

[6] L. Fan, C. Zhu, Z. Miao, and M. Hu, "Modal analysis of a DFIG-based wind farm interfaced with a series compensated network," *IEEE Trans. Energy Convers.*, vol. 26, no. 4, pp. 1010–1020, Dec. 2011.

[7] J. Yao, X. Wang, J. Li, R. Liu, and H. Zhang, "Sub-synchronous resonance damping control for series-compensated DFIG-based wind farm with improved particle swarm optimization algorithm," *IEEE Trans. Energy Convers.*, vol. 34, no. 2, pp. 849–859, Jun. 2019.

[8] M. A. Chowdhury and G. M. Shafiullah, "SSR mitigation of series-compensated DFIG wind farms by a nonlinear damping controller using partial feedback linearization," *IEEE Trans. Power Syst.*, vol. 33, no. 3, pp. 2528–2538, May 2018.

[9] P. Li, J. Wang, L. Xiong, and M. Ma, "Robust nonlinear controller design for damping of sub-synchronous control interaction in DFIG-based wind farms," *IEEE Access*, vol. 7, pp. 16626–16637, 2019.

[10] P. Li, L. Xiong, F. Wu, M. Ma, and J. Wang, "Sliding mode controller based on feedback linearization for damping of sub-synchronous control interaction in DFIG-based wind power plants," *Int. J. Electr. Power Energy Syst.*, vol. 107, pp. 239–250, May 2019.

[11] P.-H. Huang, M. S. El Moursi, W. Xiao, and J. L. Kirtley, "Subsynchronous resonance mitigation for series-compensated DFIG-based wind farm by using two-degree-of-freedom control strategy," *IEEE Trans. Power Syst.*, vol. 30, no. 3, pp. 1442–1454, May 2015.

[12] A. E. Leon and J. A. Solsona, "Sub-synchronous interaction damping control for DFIG wind turbines," *IEEE Trans. Power Syst.*, vol. 30, no. 1, pp. 419–428, Jan. 2015.

[13] H. A. Mohammadpour, A. Ghaderi, and E. Santi, "Analysis of subsynchronous resonance in doubly-fed induction generator-based wind farms interfaced with gate–controlled series capacitor," *IET Gener., Transmiss. Distrib.*, vol. 8, no. 12, pp. 1998–2011, Dec. 2014.

[14] L. Fan and Z. Miao, *Modeling and Analysis of Doubly Fed Induction Generator Wind Energy Systems*. New York, NY, USA: Academic, 2015.

[15] H. A. Mohammadpour and E. Santi, "Analysis of sub-synchronous resonance (SSR) in doubly-fed induction generator (DFIG)-based wind farms," *Synth. Lectures Power Electron.*, vol. 5, no. 3, pp. 1–64, Sep. 2015.

[16] L. Fan, R. Kavasseri, Z. L. Miao, and C. Zhu, "Modeling of DFIG-based wind farms for SSR analysis," *IEEE Trans. Power Del.*, vol. 25, no. 4, pp. 2073–2082, Oct. 2010.

[17] M. Wu and L. Xie, "Calculating steady-state operating conditions for DFIG-based wind turbines," *IEEE Trans. Sustain. Energy*, vol. 9, no. 1, pp. 293–301, Jan. 2018.

[18] I. S. W. Group, "First benchmark model for computer simulation of subsynchronous resonance," *IEEE Trans. Power App. Syst.*, vol. PAS-96, no. 5, pp. 1565–1572, Sep. 1977.

[19] L. Fan and Z. Miao, "Mitigating SSR using DFIG-based wind generation," *IEEE Trans. Sustain. Energy*, vol. 3, no. 3, pp. 349–358, Jul. 2012.

[20] H. A. Mohammadpour and E. Santi, "SSR damping controller design and optimal placement in rotor-side and grid-side converters of series-compensated DFIG-based wind farm," *IEEE Trans. Sustain. Energy*, vol. 6, no. 2, pp. 388–399, Apr. 2015.

[21] M. Abdeen, H. Li, and L. Jing, "Improved subsynchronous oscillation detection method in a DFIG-based wind farm interfaced with a series-compensated network," *Int. J. Electr. Power Energy Syst.*, vol. 119, Jul. 2020, Art. no. 105930.

[22] L. Piyasinghe, Z. Miao, J. Khazaei, and L. Fan, "Impedance model-based SSR analysis for TCSC compensated type-3 wind energy delivery systems," *IEEE Trans. Sustain. Energy*, vol. 6, no. 1, pp. 179–187, Jan. 2015.

[23] Y. Lei, A. Mullane, G. Lightbody, and R. Yacamini, "Modeling of the wind turbine with a doubly fed induction generator for grid integration studies," *IEEE Trans. Energy Convers.*, vol. 21, no. 1, pp. 257–264, Mar. 2006.

[24] F. Mei and B. Pal, "Modal analysis of grid-connected doubly fed induction generators," *IEEE Trans. Energy Convers.*, vol. 22, no. 3, pp. 728–736, Sep. 2007.

[25] S. Tohidi, H. Oraee, M. R. Zolghadri, S. Shao, and P. Tavner, "Analysis and enhancement of low-voltage ride-through capability of brushless doubly fed induction generator," *IEEE Trans. Ind. Electron.*, vol. 60, no. 3, pp. 1146–1155, Mar. 2013.

MOHAMED ABDEEN received the B.Sc. and M.Sc. degrees in electrical engineering from Al-Azhar University, Cairo, Egypt, in 2011 and 2016, respectively, and the Ph.D. degree from Chongqing University, Chongqing, China, in 2020. He is currently an Assistant Professor with the Department of Electrical Engineering, Al-Azhar University. His research interests include power system stability, optimization, and control.

HUI LI received the M.Eng. and Ph.D. degrees in electrical engineering from Chongqing University, Chongqing, China, in 2000 and 2004, respectively. From 2005 to 2007, he was a Postdoctoral Research Fellow with the Institute of Energy Technology, Aalborg University, Denmark. Since 2008, he has been a Professor with the Department of Electrical Machinery and Electrical Apparatus, School of Electrical Engineering, Chongqing University. He is currently a Researcher with the State Key Laboratory of Equipment and System Safety of Power Transmission and Distribution and New Technology. His main research interests include wind power generation, and design and control of electrical machines.

SALAH KAMEL received the International Ph.D. degree from the University of Jaen, Spain (Main) and Aalborg University, Denmark (Host), in January 2014. He is currently an Associate Professor with the Department of Electrical Engineering, Aswan University. He is also a Leader of the Advanced Power Systems Research Laboratory (APSR Lab), Power Systems Research Group, Aswan, Egypt. His research interests include power system analysis and optimization, smart grid, and renewable energy systems.

AHMED KHALED received the B.Sc. and M.Sc. degrees in electrical engineering from Al-Azhar University, Qena, Egypt, in 2011 and 2017, respectively. He is currently pursuing the Ph.D. degree with Chongqing University, Chongqing, China. His research interests include renewable energy and power system control.

MAHMOUD EL-DABAH received the B.Sc., M.Sc., and Ph.D. degrees from the Faculty of Engineering, Al-Azhar University, Cairo, Egypt, in 2007, 2012, and 2016, respectively. He is currently a Professor Assistant with the Department of Electrical Engineering, Faculty of Engineering, Al-Azhar University. His research interests include power system operation, control, and planning, applications of modern optimization techniques in electric power systems, renewable energy sources, power system stability, and distributed power generation.

MOHAMMED KHARRICH was born in Fez, Morocco, in 1989. He received the B.S. degree in mechanical engineering from Sidi Mohamed Ben Abdellah University, Fez, in 2011, and the M.S. degree in mechatronics engineering from Abdelmalek Essaâdi University, Tetouan, in 2014. He is currently pursuing the Ph.D. degree in electrical engineering with the Mohammadia School of Engineering, Mohammed V University, Rabat, Morocco. He has published many articles in international journals and conferences. His research interests include microgrid systems, modeling, simulation, and optimization of renewable and conventional power systems, metaheuristic algorithms, and developing and application of stochastic and metaheuristic algorithms. He is also a reviewer of many highly indexed journals.

HATEM FAIZ SINDI (Senior Member, IEEE) received the B.Sc. degree in electrical engineering from King Abdulaziz University, Jeddah, Saudi Arabia, in 2007, and the M.Sc. and Ph.D. degrees in electrical engineering from the University of Waterloo, Waterloo, ON, Canada, in 2013 and 2018, respectively. He is currently an Assistant Professor with the Department of Electrical and Computer Engineering, King Abdulaziz University. His research interests include smart grid, renewable DG, distribution system planning, electric vehicles, storage systems, and bulk power system reliability.

● ● ●